Effects of *in vivo* cyclic compressive loading on the distribution of local type II collagen and superficial lubricin in rat knee articular cartilage

XIANG JI
Kyoto University
Akira Ito (ito.akira.4m@kyoto-u.ac.jp)
Kyoto University https://orcid.org/0000-0002-9645-9777
Akihiro Nakahata
Kyoto University
Kohei Nishitani
Kyoto University
Hiroshi Kuroki
Kyoto University
Tomoki Aoyama
Kyoto University

Research article

Keywords: In vivo cyclic compression, Post-traumatic osteoarthritis, Cartilage degeneration, Rat model, Type II collagen, Superficial lubricin

Posted Date: December 26th, 2019

DOI: https://doi.org/10.21203/rs.2.19640/v1

Abstract

Background

This study aimed to examine the effects of a single episode of in vivo cyclic loading on rat knee articular cartilage (AC) in mid-term observation and investigate relevant factors associated with the progression of post-traumatic osteoarthritis (PTOA).

Methods

Twelve-week-old Wistar rats underwent one episode of 60 cycles of dynamic compression of 20 N or 50 N on their right knee joint. The spatiotemporal changes in the AC after loading were evaluated using histology and immunohistochemistry at 3 days, 1, 2, 4 and 8 weeks after loading (n=6 for each condition). The chondrocyte vitality was assessed at 1, 3, 6 and 12 hours after loading (n=2 for each condition).

Results

A localized AC lesion on lateral femoral condyle was confirmed in all subjects. The surface and intermediate cartilage in the affected area degenerated after loading, yet the calcified cartilage remained intact. The expression of type II collagen in the lesion cartilage was upregulated after loading, whereas the superficial lubricin layer was eroded in response to cyclic compression. However, the distribution of superficial lubricin gradually recovered to the normal level 4 weeks after loading-induced injury.Conclusion

We confirmed that 60 times cyclic loading exceeding 20 N could result in cartilage damage in rat knee. Endogenous repairs in well-structured joints work well with rebuilding protective layers on the lesion cartilage surface, which could be the latent factor in delaying the progression of PTOA.

Background

Post-traumatic osteoarthritis (PTOA) is a classification of clinical osteoarthritis (OA) which is more common among patients who have a history of articular cartilage (AC) damage and ligament injury. Animal models play an important role in understanding the pathophysiology of and developing novel treatments for PTOA. Small animals like rodents, have an advantage of a faster pathological process and have lower maintenance costs in comparison to large animals, and hence, are widely used as PTOA models for experimental purpose. The anterior cruciate ligament transection (ACLT) and destabilization of medial meniscus (DMM) have been the optimal options for short term studies since past. In the recent decades, non-surgical models were alternatively taken into account in order to avoid surgery-induced inflammation that could affect the results of evaluation. One of the most promising candidates is the cyclic compression on knee AC [1].

The in vivo cyclic compression model was first designed for verifying trabecular bone adaptation to mechanical loading [2–4], and was developed as a nonsurgical model of OA in later studies [5–12]. However, there are still some doubts whether these models can appropriately simulate the pathologic progression of clinically relevant secondary OA. One problem was the over-frequent loading, which contributed to excessive subchondral bone reaction and the formation of disproportionately giant osteophytes reported in many cases [7–8, 12]. Ko et al [11] reported a single session of loading induced OA-like morphological destruction, whereas the regimen comprised 1200 cycles, which was roughly equal to the 5 days/week design in other studies. Poulet et al [5] confirmed a loading episode of 60 cycles induced AC lesion without osteophyte formation, yet after tracing it for 2 weeks found no loss of safranin O staining. Therefore, further study of long-term tracking of low dose loading effectiveness is necessary.

Although earlier studies using cyclic compression models illustrated visible osteophytes and declined substrate staining, none of them have reported the irregular wearing of cartilage surface or subchondral bone porosity loss, which were considered as important characteristics of OA progression in surgery-induced rodent OA models [13–14]. Thus, depending on the magnitude of compulsive loading and the methodology of joint instability surgery, the mechanism of repair or alleviation of the AC lesion in OA progression are still unclear.

Therefore, the current study aimed to track the relatively long-term effect of in vivo low dose cyclic loading on rat knee joint, which is the first such study in rat species. Secondly, we examined changes over time in loading-affected cartilage and investigated the potential reason why OA development in non-surgical model progresses slower than in a surgery model.

Methods

Mechanical Loading procedures and sample allocation

All experimental procedures were approved by the animal research committee of Kyoto University (approval number: Med kyo 17616). Seventy-four 12-week-old wild type male Wistar rats were used in the study. The animals were anesthetized with 5% Isoflurane solution (Pfizer, Tokyo, Japan) before being injected intraperitoneally with 1 μg/g somnopentyl (Kyoritsu Seiyaku Corp., Tokyo, Japan). Each animal's right knee was fixed with a customized cup with approximately 140 degrees flexion as previously described [6] and subjected to one session of dynamic loading in the daytime using a measurable compressive instrument (Autograph AG-X, Shimazu, Japan). The loading regimen included a preload of 5 N, peak load of 20 N or 50 N with approaching speed of 1 mm/s and 10 s rest intervals (Fig. 1A,1B). The load levels were set according to previous studies in other species [6, 9], which was proportionately amplified based on the animal weight. Each session comprised 60 cycles that lasted about 12 min. After loading compression, animals were returned to transparent plastic cages with a 12-h light/dark cycle and provided with sufficient feed and free space for movement. Experimental rats were randomly divided into three groups (peak load 20 N, 50 N and control). The rats (n = 6 for each condition, n = 60 in total) were sacrificed for histological analysis at 3 days, 1, 2, 4 and 8 weeks after compression. Knee samples that

underwent 20 N loading were harvested at 1, 3, 6 and 12 h, for the live/dead assessment of chondrocytes (n = 2 for each timepoint, n = 8 in total). The normal 12-week old Wistar rat samples served as controls (n = 4) for historical analysis and controls (n = 2) for cell viability evaluation (Fig. 1C). The randomization was addressed using Excel functions, and animals in the different experimental groups were treated in time order.

Live/dead analysis of chondrocytes

To evaluate the live/dead spatiotemporal changes of chondrocytes on lateral femoral condyles, calcein AM/ethd-1 staining (LIVE/DEAD Viability/Cytotoxicity Kit, Thermo Fisher Scientific, Tokyo, Japan) was performed immediately after the specimens were dissected from the knee joints. The samples were treated with calcein AM (diluted 1:500) and Ethd-1 (diluted 1:4000) solutions in PBS for 20 min at room temperature. The samples were then rinsed in PBS and cut into two parts alone femoral intercondylar sulcus. The lateral half was then mounted on a transparent plate with the femoral condyle towards the camera (Supplementary Fig. 1). Fluorescence micrographs were taken using a fluorescence microscope (Fluoview FV10i, Olympus, Tokyo, Japan) in FITC (495 nm/519 nm) and PI (535 nm/617 nm) channels. Live cells were indicated by green fluorescence and the dead cells by red fluorescence. Contralateral limbs harvested at 12 h were used as controls.

Histological analysis

Knee joints were fixed in 4% paraformaldehyde overnight and decalcified in 10% EDTA for 25 days. The samples were then embedded in paraffin. Twelve 6 μm sagittal sections for every 100 μm intervals were prepared which covered the entire area of the lesion in the lateral femur for each sample. Safranin O, fast green and hematoxylin staining were performed on each section and the average modified Mankin score [15] was calculated to evaluate the degree of cartilage degeneration of the lateral femoral condyle. To assess the volume of degenerative cartilage, the lesion area was defined using the image-J software and the stacked volume was calculated by multiplying the total area by 100 μm average thickness. The intensity of Safranin O staining was calculated on an inverted 8-bit grey scale image using image-J software. The relative intensity in lesion areas were calculated by dividing intensity in normal cartilage (Supplementary Fig. 2). Moreover, the hematoxylin-stained nuclei of chondrocytes in the lesion cartilage were counted.

Immunohistochemistry and semi-quantitative evaluation

Immunohistochemical staining of type II collagen (Fine Chemical Co., Toyama, Japan; Diluted 1:200), Matrix metalloproteinase thirteen (MMP-13) (ab39012 Abcam Co., Tokyo, Japan; Diluted 1:1000), A disintegrin and metalloproteinase with thrombospondin motifs five (ADAMTS-5) (ab185795 Abcam Co., Tokyo, Japan; Diluted 1:50) and Lubricin/Proteoglycan4 (EMD Millipore, Temecula, USA; Diluted 1:1000) were performed as described below. Deparaffinized sections were treated with 3% hydrogen peroxide solution for 30 min. Then, the sections to be stained for the anti-type II collagen reaction were treated with 1.25% hyaluronidase for 60 min at room temperature. The sections for the ADAMTS-5 reaction were

treated with HistoVT one solution (Nacalai Tesque, Inc., Kyoto, Japan; diluted 1:10) for 40 min at 65 ℃. After rinsing in PBS, non-specific reaction was suppressed by blocking with 5% normal goat serum for 60 min. Subsequently, the sections were treated with primary antibodies and incubated at 4 ℃ overnight. Sections were then washed in PBS and treated with goat anti-rabbit IgG (MMP-13 and ADAMTS-5) or goat anti-mouse IgG (type II collagen and lubricin) for 30 min at room temperature. Detection was performed using the streptavidin–biotin–peroxidase complex technique with an Elite ABC kit (diluted 1:100; Vector Laboratories, Burlingame, CA, USA). Localization was detected using 3,3-diaminobenzidine solution (Vector Laboratories) followed by counterstaining with hematoxylin.

The immunohistological staining in the cartilage matrix of type II collagen and lubricin were evaluated using image-J software. Images were converted into greyscale (0–255) from dark to bright, the intensity was calculated by subtracting the values in blank spaces. (The details of ROI selection are described in supplementary Fig. 3) The number of MMP-13 and ADAMTS-5 positive immunostained chondrocytes in the lesion area and the adjoining zone were counted and normalized by dividing with the corresponding cartilage surface length. The adjoining zone was defined as the area in proximity to the lesion cartilage in a 0.48 mm × 0.64 mm 200-fold histological image.

Statistical analysis

Statistical analyses were performed using SPSS software (version 22.0; SPSS Inc., Chicago IL). Two-way Analysis of variance was employed to analyze histological staining with loading as intragroup factors and duration as intergroup factors. The normality of all continuous data was examined using the Shapiro–Wilk normality tests. The parametric variables of the modified Mankin score, volume of degenerative areas and the semi-quantitative measurements of immunohistochemistry were included in the model directly, whereas the nonparametric variables were first transformed into ranked data and then introduced into the model. Comparisons between intergroup marginal means using Tukey HSD tests were performed only when main effects exhibited significant results. As the analysis showed interactional effects in addition to the significant main effects, multiple one-way ANOVA tests with post-hoc comparisons for stratified samples were conducted on each level to examine potential differences in interactional effects among the levels. Additionally, Mann-Whitney U (2 groups) or Kruskal-Wallis H tests (3 groups) were applied to compare the control and loaded samples. The required sample size was calculated based on our pilot experimental data of lesion area size between groups. P-value < 0.05 was considered statistically significant.

Results

Vitality of the chondrocytes after cyclic loading

Samples that underwent 20 N cyclic compression were tested by calcein AM/ethd-1 staining. (Fig. 2) The representative images exhibited mixed distribution of red and green fluorescent cells at 1 and 3 h after loading, whereas large areas without green-stained chondrocytes were observed at the time points of 6 and 12 h, indicating that complete cell death occurred within 6 h even at the lower load level of 20 N.

Degree and extension of articular cartilage lesion

Histology showed that AC in both groups were damaged, and one focal degenerative zone in lateral femoral condyle was confirmed for every subject (Fig. 3A). However, the AC surface remained intact except for a slight fibrillation present in several samples (data not shown). A clear boundary between the lesion cartilage and unaffected calcified cartilage could be observed 2 weeks after loading. Average modified Mankin score per section increased after loading (Fig. 3F) and differed between groups and observational durations (Fig. 3B). As the peak load or interval time increased, the degree of degeneration tended to worsen at higher histological scores (Fig. 3B). Although the lesion area volume did not change significantly throughout the duration of the study, it was significantly higher in the 50 N load group than the 20 N group at all time points (Fig. 3C). The relative Safranin O staining intensity in the lesion area declined with time after loading both groups in comparison to the intact area (Fig. 3D); however, there was no evident difference between groups with 20 N or 50 N peak loads. In addition, the number of hematoxylin stained nuclei in the lesion area continuously decreased after loading in both groups (Fig. 3E 3G), whereas, no significant changes were found in midterm observation from 2 to 8 weeks.

Expression of type II collagen in the lesion area

Immunohistochemistry results illustrated focal type II collagen overexpression in the AC lesion. Enhanced staining was observed in each sample in comparison to adjacent intact substrates (Fig. 4A), and the intensity in loaded samples was significantly higher than the control group (Fig. 4B). However, there were no notable effects on intensity in the lesion region with different load levels or time points (Fig. 4C, 4D), when compared using either raw values or relative percentage increments.

Distribution of ADAMTS-5 and MMP-13 positive chondrocytes

Superficial and intermediate zone chondrocytes in the control group moderately expressed MMP-13 and ADAMTS-5 (Supplementary Fig. 4). In the loading groups, we found positively stained radial zone chondrocytes under the lesion area (Fig. 5, 6), which were not observed in normal samples (quantitative data not shown). The number of active cells in the area adjoining the lesion (no direct contact) significantly increased after loading in comparison to normal AC (Fig. 5B, 6B). Moreover, the results of semi-quantitative analysis revealed that the number of both MMP-13 and ADAMTS-5 positive chondrocytes (in the lesion area or in the adjoining region) gradually decreased during the 8-weeks of observation (Fig. 5C, 5D, 6C, 6D). However, no significant main effects were generated by load levels.

Superficial lubricin response to cyclic loading

Lubricin expression in the lateral femoral condyle AC is presented in Fig. 7. The staining intensity in the lesion area of substrates within the superficial cartilage declined 1 week after loading compared to the intact area (Fig. 7A). However, semi-quantitative analyses showed an increased concentration of lubricin

on the AC lesion over time, which reached the same level at the time points of 4 and 8 weeks in comparison to the intact area (Fig. 7B). No statistical load level effect was found, whereas main effects of duration and interaction between observational duration and load effect were confirmed. Furthermore, results of stratified analysis revealed that superficial lubricin in 20 N loaded samples were more likely to recover (more pairwise differences) in comparison to 50 N samples (Fig. 7C, 7D). Additionally, we found the signs of staining aggregating around the site of degenerative chondrocytes or even the lacunae from dead cells without hematoxylin-stained nuclei.

Discussion

The current study demonstrated for the first time that a single episode of 60 cycles of mechanical stimuli can induce AC lesion in the lateral femoral condyle of rat, which is consistent with the results reported in smaller rodents like mouse [5–6]. The scope and localization of the lesion area were relatively steady in both the high and low load level groups as estimated by the chondrocyte-degenerative volume in each sample with low cartilage structural destruction except mild fibrillation in rare samples. However, the histological scores deteriorated over time due to the Safranin O staining loss and diffused hypocellularity in the affected area [15]. ADAMTS-5, which is reportedly the primary catalyst for aggrecan degradation [16], was found to be overexpressed immediately after AC injury in the current study (Fig. 5). However, the Safranin O stained substances continued to degrade whereas the ADAMTS-5 expression dropped to normal levels after 4 weeks. Furthermore, the affected chondrocytes in the direct contact area did not demonstrate a positive response (Fig. 5). Studies on cell signaling have considered that overloading will activate the toll-like receptors expressed on chondrocytes, resulting in the release of proteinases and inflammatory cytokines [17]. However, our results showed that color fading only occurred in the central region of cell death but not in the adjoining positive cells area. These results suggested that the aggrecanase of ADAMTS-5 might combine with other factors to augment proteoglycan degradation. We assumed that the integrity of fibrillar collagen networks or chondrocyte vitality may also play important roles in the maintenance of aggrecan homeostasis, which needs to be investigated in the future. Moreover, there was a distinct difference of staining between AC above and below the tidemark (Fig. 3A), which were consistent with the in vitro results that calcified radial zones of cartilage suffered less than 5% of the total mechanical stress [18–19].

The PTOA models of ACLT and DMM, which induced instability of the entire joint or deflection of load bearing towards medial or lateral tibial compartment, were widely used in rodents for short-term studies. The histological characteristics were defined as gradually developing chondrocyte apoptosis and cartilage matrix loss [20]. However, we did not find any apoptotic cell around the lesion area even at very early observation of 6 h after loading (data not shown), which was considerably different from the previous results in mouse that illustrated that clustered active chondrocytes by TUNEL staining were retained in degenerative AC until 14 days after loading [6]. Our results of live/dead staining demonstrated that chondrocytes in the superficial lesion cartilage were dead within 6 h by direct damage (Fig. 2). In this study, we set up the loading routine based on the weight ratio between rat and mouse as indicated in previous studies, which may have led to results slightly different from the previous study. We quantified

the size of the lesion area and found that the volume containing degenerative chondrocytes had not changed much between each time point for both groups. However, the decreased Safranin O staining area enlarged over time that indicated the gradual depletion of glycosaminoglycans in the chondrocyte death region after loading. On the other hand, the AC shape destruction did not progress as rapidly as the invasive models, which illustrated jagged cartilage surface and subchondral bone perforation within 4 weeks after instability surgery [21–22]. According to our investigation, this non-surgical model may be better for the simulation of acute extensive AC damage, which is more common in the field of sport injuries.

Expression of Col2 was found to be transiently increased within 1 h after ex vivo mechanical loading in several experiments using extracted cartilage explants [23–24]. In the tissue engineering field, a recently published review [25] summarized biochemical anabolism of synthetic substrate-seeded chondrocytes subjected to in vitro dynamic loading, most of which demonstrated subsequent results of Col2 upregulation in response to varied loading regimens. Ragan PM [23] reported transient upregulation of type-II collagen within 4 h in extracted bovine cartilage explants subjected to static mechanical compression, but did not check the chondrocytes survival rate. The current study, to our knowledge, is a first report of focal enhanced staining of type II collagen on lesion cartilage which has undergone in vivo cyclic loading, even with the complete death of the affected surface chondrocytes within 6 h. A previous study reported decreased Safranin O and Col2 staining in an osteochondral defect model [26], which was directly created on the AC surface using a 1-mm biopsy punch. However, our model illustrated diametrically opposite Type II collagen response to cyclic loading. Although one of the major collagenases, MMP-13 overexpressed immediately after loading injury (Fig. 6), the morphological degradation of AC did not progress extensively as in regular OA development. Further studies should focus on whether type II collagen proliferation is beneficial or harmful to AC protection.

The lubricin localized in the cartilage surface is reportedly a protective and lubricating component of the O-linked glycoprotein [27]. We found that superficial lubricin staining in the damaged area decreased drastically immediately after cyclic loading in comparison with the non-loaded region (Fig. 7). A decreased superficial cartilage lubricin/proteoglycan 4 level was confirmed in both in vivo [28] and ex vivo [29] experiments. Several studies have reported increased coefficient of friction within few hours of cyclic loading [30–31], and also that lubricin in the cartilage surface was denuded by loading, even in the joint where most chondrocytes remained alive throughout the observation period [31]. Our study revealed similar results in a non-surgical model at early observation after in vivo cyclic compression, whereas the results of immunohistochemistry illustrated that cartilage surface lubricin staining diminished only in the lesion area where cell death occurred. Further studies should provide more quantitative data and explore if superficial lubricin depleted independently of the factor of cell death. On the other hand, in the experimental sheep [32–33] and horse [34–35] models, lubricin concentration in the synovial fluid was upregulated transiently at the acute phase after injury, and synovial PRG4 (The gene encodes Lubricin) expression presented positive correlation with TNFα and ADAMTS-5 [35]. Our results similarly illustrated that cleavage products of MMP-13 and ADAMTS-5 mounted dramatically within 1 week after trauma and dropped to the basal level gradually (Fig. 5, 6). Further investigations should also focus on synovium

response and check if in vivo cyclic loading will promote or inhibit the synovial cell secretion of intra-articular lubricin.

Meanwhile, after tracking different time points within 8 weeks, we found that superficial cartilage staining with lubricin gradually recovered to the normal level (Fig. 8). The results after 4 weeks indicated a different direction of OA progression compared to those with joint instability-induced OA. Although, lubricin expression on cartilage was found elevated in late-stage OA patients [36], the mainstream results on the posttraumatic OA of human [37] and animal joint instability models [28, 38–40] in a long-term observation demonstrated that the joint lubricin concentration decreased after injury or surgery. Combining the results of decreased Prg4 expression in unstable joint after forced movement [41–42] with our results, we hypothesized that the instability-induced persistent incentives should play a more important role than the magnitude of loading in determining irreversible lubricin loss. Several studies [39, 43–44] where exogenous recombinant lubricin was delivered to medial meniscectomized rats found that the cartilage surface protein was prevented from depletion in the experimental group. In the current study, we found a self-healing process in the loading-damaged AC without any lubricin supplementation, which indicates that endogenous lubricin is an important repair mechanism in the post-traumatic knee and provides a plausible explanation that the cartilage degradation progression of non-invasive loading model was slower than joint instability surgery models. Interestingly, although superficial cell death was confirmed completely within 6 h after loading, the locations of cartilage lacunae were strongly stained with lubricin even at 8 weeks after injury. Previous studies found chondrocytes encapsulated in agarose [19, 45] and cartilage explants [46] expressed higher prg4 gene subject to compressive strain, and the intensified lacunae staining around cells were confirmed in the immunofluorescence images [19], which is similar to our results. Further studies should focus on potential links between chondrocyte-derived lubricin and the mechanism of superficial cartilage repairment.

The current study has some limitations. First, it focused on investigating the mid-term changes over time from 3 days to 8 weeks after loading implementation. Since cell death, type II collagen biosynthesis and superficial lubricin degradation happened earlier than our expectation, further studies should more precisely design the unit of observation intervals in hours to disclose the full process of dynamic loading-induced cellular reaction. Second, we did not examine the synovial changes in response to loading. As we described above, upregulated inflammatory cytokines and PRG4 expression were found in multiple researches, which possibly induced the changes of microenvironment in the joint cavity, and weakened the significance of the antigen detection results in the AC. For instance, the results like the increase of cartilage surface-adhesive protective proteins like lubricin could be confused by the higher secretion of lubricin in synovial fluid after injury, which gives rise to the question whether lubricin recovery could ascribe to self-healing capabilities or is simply due to high concentration of lubricin in the environment. Study in the future should evaluate the synovium using quantitative techniques to eliminate internal interference factors. Third, in the current study, we only assessed the cartilage lesion on lateral femur condyle. The cartilage damage on the other contact surface of lateral tibia should be examined in the future. Last, we failed to compare the current model to any surgery-induced model. As we described above, the surface lubricin reportedly diminished in many injury-induced OA animals [28, 38–40], whereas

it is still unknown if the factor of joint instability independently affected the progression of post-traumatic OA, especially in the lesion area. Further studies should combine invasive destabilization surgery to pre-existing lesion caused by cyclic compression, which could reflect the spatiotemporal changes of cartilage in the non-contact area.

In conclusion, we found a specific-localized AC lesion in both the 20 N and 50 N groups that underwent 60 cycles of compression in rat knee joints. The size of lesion was affected by the load level and the intensity of histological staining weakened with time after loading. The local expression of type II collagen was raised after repeated loading whereas lubricin in the cartilage surface was lost in response to cyclic compression. However, the distribution of superficial lubricin recovered at 4 weeks after non-surgical injury (Fig. 8). These results indicated that dynamic loading exceeding 20 N could damage the lateral femoral condyle AC in rat. Although the damage caused localized chondrocyte deaths and upregulated expression of degrading enzymes, endogenous repairments in well-structured joint worked by rebuilding the layer of protective proteins on the superficial cartilage.

List Of Abbreviations

AC: Articular cartilage

PTOA: Post-traumatic osteoarthritis

ACLT: Anterior cruciate ligament transection

DMM: Destabilization of medial meniscus

MMP-13: Matrix metalloproteinase thirteen

ADAMTS-5: A disintegrin and metalloproteinase with thrombospondin motifs five

Declarations

Ethics approval and consent to participate

All experimental procedures were approved by the animal research committee of Kyoto University (approval number: Med kyo 17616).

Consent for publication

Not applicable.

Availability of data and materials

All data generated or analysed during this study are included in this published article and its supplementary information files.

Competing interests

The authors declare no competing interests.

Funding

This study was supported in part by a JSPS KAKENHI Grant, number JP18H03129 and JP18K19739.

Acknowledgments

None

Author Contributions

XJ: conception and design of the study, acquisition, analysis, and interpretation of data, drafting of the article, revision of the article, final approval of the article.

AI: conception and design of the study, interpretation of data, drafting of the article, revision of the article, final approval of the article.

AN: conception and design of the study, interpretation of data, revision of the article, final approval of the article.

KN: conception and design of the study, interpretation of data, revision of the article, final approval of the article.

HK: obtaining of funding, conception and design of the study, interpretation of data, revision of the article, final approval of the article.

TA: conception and design of the study, interpretation of data, revision of the article, final approval of the article.

References

1. Kuyinu EL, Narayanan G, Nair LS, Laurencin CT. Animal models of osteoarthritis: classification, update, and measurement of outcomes. J Orthop Surg Res 2016; 11: 19.
2. De Souza RL, Matsuura M, Eckstein F, Rawlinson SC, Lanyon LE, Pitsillides AA. Non-invasive axial loading of mouse tibiae increases cortical bone formation and modifies trabecular organization: a new model to study cortical and cancellous compartments in a single loaded element. Bone 2005; 37: 810-818.
3. Holguin N, Brodt MD, Sanchez ME, Kotiya AA, Silva MJ. Adaptation of tibial structure and strength to axial compression depends on loading history in both C57BL/6 and BALB/c mice. Calcif Tissue Int 2013; 93: 211-221.

4. Lynch ME, Main RP, Xu Q, Walsh DJ, Schaffler MB, Wright TM, et al. Cancellous bone adaptation to tibial compression is not sex dependent in growing mice. J Appl Physiol (1985) 2010; 109: 685-691.
5. Poulet B, Hamilton RW, Shefelbine S, Pitsillides AA. Characterizing a novel and adjustable noninvasive murine joint loading model. Arthritis Rheum 2011; 63: 137-147.
6. Wu P, Holguin N, Silva MJ, Fu M, Liao W, Sandell LJ. Early response of mouse joint tissue to noninvasive knee injury suggests treatment targets. Arthritis Rheumatol 2014; 66: 1256-1265.
7. Lockwood KA, Chu BT, Anderson MJ, Haudenschild DR, Christiansen BA. Comparison of loading rate-dependent injury modes in a murine model of post-traumatic osteoarthritis. J Orthop Res 2014; 32: 79-88.
8. Ko FC, Dragomir C, Plumb DA, Goldring SR, Wright TM, Goldring MB, et al. In vivo cyclic compression causes cartilage degeneration and subchondral bone changes in mouse tibiae. Arthritis Rheum 2013; 65: 1569-1578.
9. Poulet B, de Souza R, Kent AV, Saxon L, Barker O, Wilson A, et al. Intermittent applied mechanical loading induces subchondral bone thickening that may be intensified locally by contiguous articular cartilage lesions. Osteoarthritis Cartilage 2015; 23: 940-948.
10. Onur TS, Wu R, Chu S, Chang W, Kim HT, Dang AB. Joint instability and cartilage compression in a mouse model of posttraumatic osteoarthritis. J Orthop Res 2014; 32: 318-323.
11. Ko FC, Dragomir CL, Plumb DA, Hsia AW, Adebayo OO, Goldring SR, et al. Progressive cell-mediated changes in articular cartilage and bone in mice are initiated by a single session of controlled cyclic compressive loading. J Orthop Res 2016; 34: 1941-1949.
12. Adebayo OO, Ko FC, Wan PT, Goldring SR, Goldring MB, Wright TM, et al. Role of subchondral bone properties and changes in development of load-induced osteoarthritis in mice. Osteoarthritis Cartilage 2017; 25: 2108-2118.
13. McErlain DD, Appleton CT, Litchfield RB, Pitelka V, Henry JL, Bernier SM, et al. Study of subchondral bone adaptations in a rodent surgical model of OA using in vivo micro-computed tomography. Osteoarthritis Cartilage 2008; 16: 458-469.
14. Iijima H, Aoyama T, Ito A, Tajino J, Nagai M, Zhang X, et al. Destabilization of the medial meniscus leads to subchondral bone defects and site-specific cartilage degeneration in an experimental rat model. Osteoarthritis Cartilage 2014; 22: 1036-1043.
15. Bomsta BD, Bridgewater LC, Seegmiller RE. Premature osteoarthritis in the Disproportionate micromelia (Dmm) mouse. Osteoarthritis Cartilage 2006; 14: 477-485.
16. Glasson SS, Askew R, Sheppard B, Carito B, Blanchet T, Ma HL, et al. Deletion of active ADAMTS5 prevents cartilage degradation in a murine model of osteoarthritis. Nature 2005; 434: 644-648.
17. Jorgensen AEM, Kjaer M, Heinemeier KM. The Effect of Aging and Mechanical Loading on the Metabolism of Articular Cartilage. J Rheumatol 2017; 44: 410-417.
18. Wong M, Carter DR. Articular cartilage functional histomorphology and mechanobiology: a research perspective. Bone 2003; 33: 1-13.

19. Jeon JE, Schrobback K, Hutmacher DW, Klein TJ. Dynamic compression improves biosynthesis of human zonal chondrocytes from osteoarthritis patients. Osteoarthritis Cartilage 2012; 20: 906-915.
20. Iijima H, Aoyama T, Ito A, Yamaguchi S, Nagai M, Tajino J, et al. Effects of short-term gentle treadmill walking on subchondral bone in a rat model of instability-induced osteoarthritis. Osteoarthritis Cartilage 2015; 23: 1563-1574.
21. Hayami T, Pickarski M, Wesolowski GA, McLane J, Bone A, Destefano J, et al. The role of subchondral bone remodeling in osteoarthritis: reduction of cartilage degeneration and prevention of osteophyte formation by alendronate in the rat anterior cruciate ligament transection model. Arthritis Rheum 2004; 50: 1193-1206.
22. Iijima H, Aoyama T, Tajino J, Ito A, Nagai M, Yamaguchi S, et al. Subchondral plate porosity colocalizes with the point of mechanical load during ambulation in a rat knee model of post-traumatic osteoarthritis. Osteoarthritis Cartilage 2016; 24: 354-363.
23. Ragan PM, Badger AM, Cook M, Chin VI, Gowen M, Grodzinsky AJ, et al. Down-regulation of chondrocyte aggrecan and type-II collagen gene expression correlates with increases in static compression magnitude and duration. J Orthop Res 1999; 17: 836-842.
24. Fitzgerald JB, Jin M, Dean D, Wood DJ, Zheng MH, Grodzinsky AJ. Mechanical compression of cartilage explants induces multiple time-dependent gene expression patterns and involves intracellular calcium and cyclic AMP. J Biol Chem 2004; 279: 19502-19511.
25. Anderson DE, Johnstone B. Dynamic Mechanical Compression of Chondrocytes for Tissue Engineering: A Critical Review. Front Bioeng Biotechnol 2017; 5: 76.
26. Yamaguchi S, Aoyama T, Ito A, Nagai M, Iijima H, Tajino J, et al. The Effect of Exercise on the Early Stages of Mesenchymal Stromal Cell-Induced Cartilage Repair in a Rat Osteochondral Defect Model. PLoS One 2016; 11: e0151580.
27. Coles JM, Zhang L, Blum JJ, Warman ML, Jay GD, Guilak F, et al. Loss of cartilage structure, stiffness, and frictional properties in mice lacking PRG4. Arthritis Rheum 2010; 62: 1666-1674.
28. Elsaid KA, Machan JT, Waller K, Fleming BC, Jay GD. The impact of anterior cruciate ligament injury on lubricin metabolism and the effect of inhibiting tumor necrosis factor alpha on chondroprotection in an animal model. Arthritis Rheum 2009; 60: 2997-3006.
29. Jones AR, Chen S, Chai DH, Stevens AL, Gleghorn JP, Bonassar LJ, et al. Modulation of lubricin biosynthesis and tissue surface properties following cartilage mechanical injury. Arthritis Rheum 2009; 60: 133-142.
30. McCann L, Ingham E, Jin Z, Fisher J. Influence of the meniscus on friction and degradation of cartilage in the natural knee joint. Osteoarthritis Cartilage 2009; 17: 995-1000.
31. Drewniak EI, Jay GD, Fleming BC, Zhang L, Warman ML, Crisco JJ. Cyclic loading increases friction and changes cartilage surface integrity in lubricin-mutant mouse knees. Arthritis Rheum 2012; 64: 465-473.
32. Barton KI, Ludwig TE, Achari Y, Shrive NG, Frank CB, Schmidt TA. Characterization of proteoglycan 4 and hyaluronan composition and lubrication function of ovine synovial fluid following knee surgery.

J Orthop Res 2013; 31: 1549-1554.

33. Atarod M, Ludwig TE, Frank CB, Schmidt TA, Shrive NG. Cartilage boundary lubrication of ovine synovial fluid following anterior cruciate ligament transection: a longitudinal study. Osteoarthritis Cartilage 2015; 23: 640-647.
34. Antonacci JM, Schmidt TA, Serventi LA, Cai MZ, Shu YL, Schumacher BL, et al. Effects of equine joint injury on boundary lubrication of articular cartilage by synovial fluid: role of hyaluronan. Arthritis Rheum 2012; 64: 2917-2926.
35. Reesink HL, Watts AE, Mohammed HO, Jay GD, Nixon AJ. Lubricin/proteoglycan 4 increases in both experimental and naturally occurring equine osteoarthritis. Osteoarthritis Cartilage 2017; 25: 128-137.
36. Neu CP, Reddi AH, Komvopoulos K, Schmid TM, Di Cesare PE. Increased friction coefficient and superficial zone protein expression in patients with advanced osteoarthritis. Arthritis Rheum 2010; 62: 2680-2687.
37. Elsaid KA, Fleming BC, Oksendahl HL, Machan JT, Fadale PD, Hulstyn MJ, et al. Decreased lubricin concentrations and markers of joint inflammation in the synovial fluid of patients with anterior cruciate ligament injury. Arthritis Rheum 2008; 58: 1707-1715.
38. Wei L, Fleming BC, Sun X, Teeple E, Wu W, Jay GD, et al. Comparison of differential biomarkers of osteoarthritis with and without posttraumatic injury in the Hartley guinea pig model. J Orthop Res 2010; 28: 900-906.
39. Flannery CR, Zollner R, Corcoran C, Jones AR, Root A, Rivera-Bermudez MA, et al. Prevention of cartilage degeneration in a rat model of osteoarthritis by intraarticular treatment with recombinant lubricin. Arthritis Rheum 2009; 60: 840-847.
40. Young AA, McLennan S, Smith MM, Smith SM, Cake MA, Read RA, et al. Proteoglycan 4 downregulation in a sheep meniscectomy model of early osteoarthritis. Arthritis Res Ther 2006; 8: R41.
41. Elsaid KA, Zhang L, Waller K, Tofte J, Teeple E, Fleming BC, et al. The impact of forced joint exercise on lubricin biosynthesis from articular cartilage following ACL transection and intra-articular lubricin's effect in exercised joints following ACL transection. Osteoarthritis Cartilage 2012; 20: 940-948.
42. Teeple E, Jay GD, Elsaid KA, Fleming BC. Animal models of osteoarthritis: challenges of model selection and analysis. Aaps j 2013; 15: 438-446.
43. Vugmeyster Y, Wang Q, Xu X, Harrold J, Daugusta D, Li J, et al. Disposition of human recombinant lubricin in naive rats and in a rat model of post-traumatic arthritis after intra-articular or intravenous administration. Aaps j 2012; 14: 97-104.
44. Jay GD, Fleming BC, Watkins BA, McHugh KA, Anderson SC, Zhang LX, et al. Prevention of cartilage degeneration and restoration of chondroprotection by lubricin tribosupplementation in the rat following anterior cruciate ligament transection. Arthritis Rheum 2010; 62: 2382-2391.

45. Nugent GE, Aneloski NM, Schmidt TA, Schumacher BL, Voegtline MS, Sah RL. Dynamic shear stimulation of bovine cartilage biosynthesis of proteoglycan 4. Arthritis Rheum 2006; 54: 1888-1896.
46. Schatti OR, Markova M, Torzilli PA, Gallo LM. Mechanical Loading of Cartilage Explants with Compression and Sliding Motion Modulates Gene Expression of Lubricin and Catabolic Enzymes. Cartilage 2015; 6: 185-193.

Figures

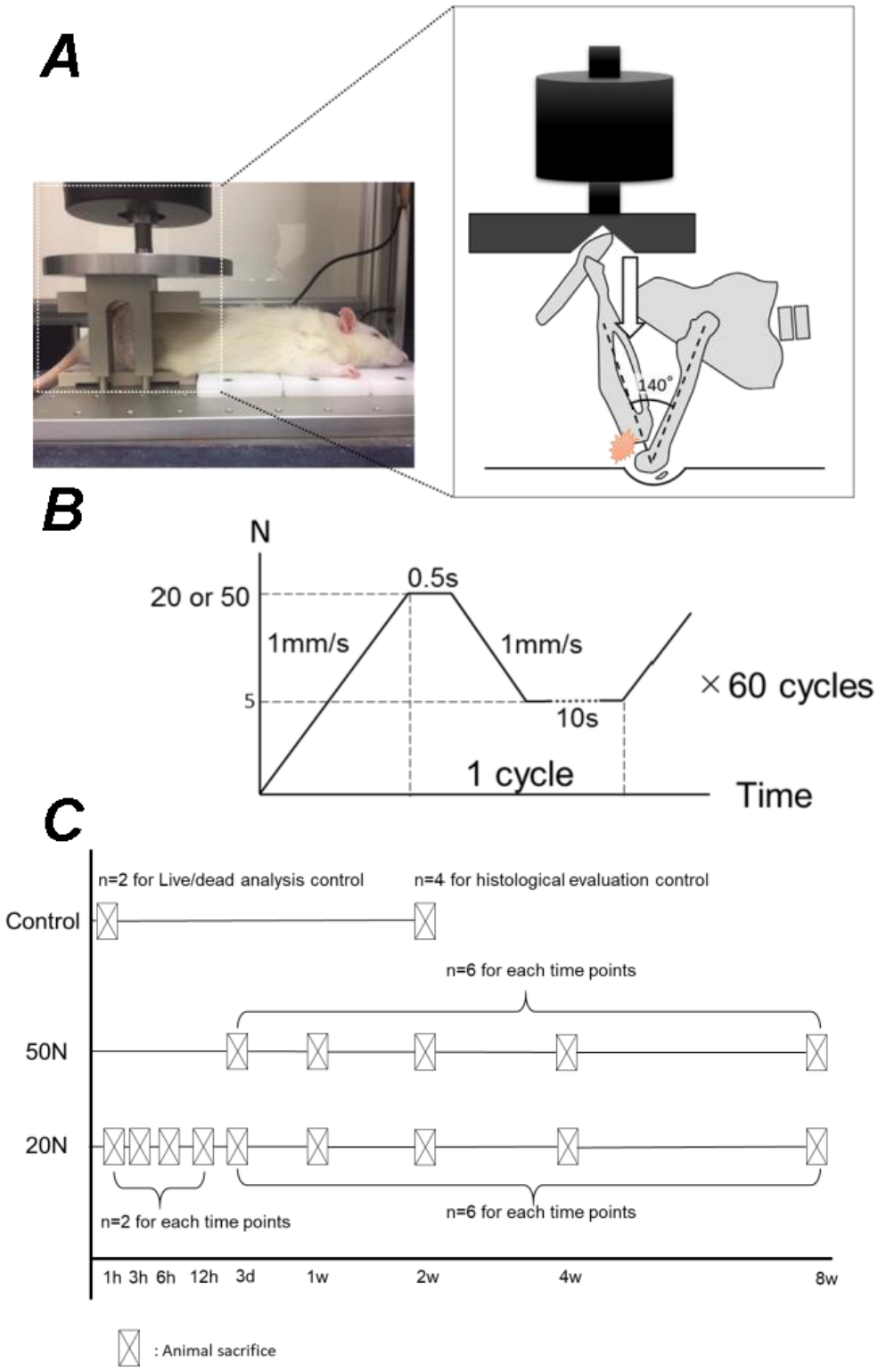

Figure 1

Schematic diagram of the non-surgical cyclic compression model. Legend: A. Right knee of anesthetized rat fixed on a customized apparatus with the patella embedded in a loading dent. The indexed knee angle was set at a deep flexion of 140°. B. A full cycle of the loading regimen contained a 0.5 s peak load and a 10 s rest interval with the loading cup approaching at a speed of 1 mm/s. The preload of 5 N and peak load of 20 N or 50 N were set for samples in corresponding groups. C. Flow chart of sample allocation.

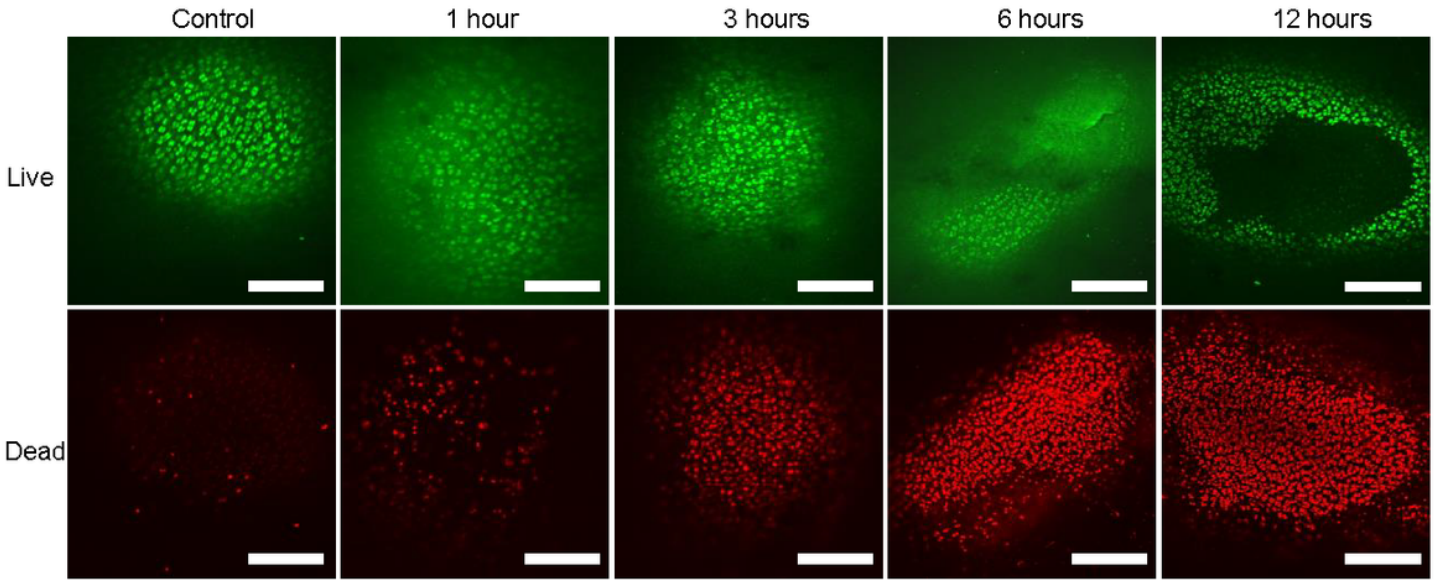

Figure 2

Chondrocyte vitality in superficial cartilage after 20 N compressive loading detection by calcein AM/ethd-1 staining. Legend: Representative fluorescent images demonstrate spatiotemporal cell death from 1 to 12 h after loading. Green and red channels illustrate the distribution of live and dead chondrocytes separately. A well-defined focal region without green-stained cells was observed at the time points of 6 and 12 h. Pre-loaded normal rats' limbs were used as control. Scale bar: 100 μm.

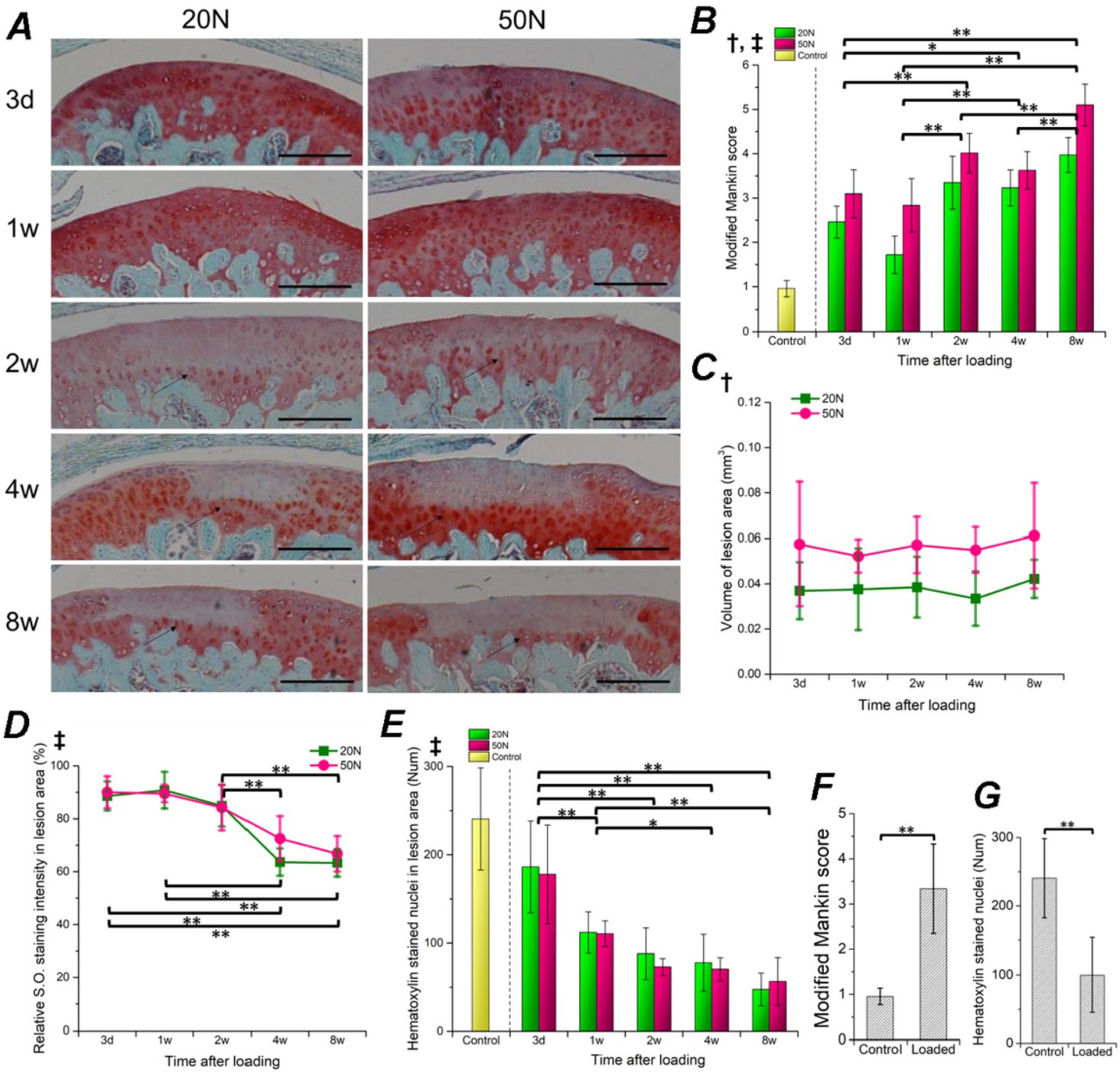

Figure 3

Effects of dynamic compression on articular cartilage in the lateral compartment of femoral condyle. Legends: A. Representative sections of Safranin O staining on the lesion area. The boundary between cartilage, above and below the tidemark, were clearly observed 2, 4 and 8 weeks after loading. Black arrows indicate a clear line between calcified cartilage and upper cartilage. B. Average modified Mankin score of 12 sagittal sections for every 100 μm intervals, which contained entire lesion areas. Larger

numbers indicate higher degree of cartilage degeneration. C. Volume of cartilage lesion with degenerative chondrocytes. Areas were depicted on 200 × fold sections using ImageJ software. D. Relative intensity of Safranin O staining in the lesion area, presented in percentage by dividing the intensity in intact area. Methodological details of C&D are described in Supplementary figure 2. E. Hematoxylin-stained chondrocytes in lesion cartilage. The numbers were normalized by dividing the surface length (mm) of cartilage. F,G. Comparison between Control (n=4) and Loaded (n=60) samples using Mann-Whitney U tests. Error bars represent standard deviation; Significant results ($p<0.05$) of two-way ANOVA analyses are presented above each chart; †: main effect of load, ‡: main effect of duration; Marginal means of each observational point were compared when ‡ was found. *$p<0.05$, **$p<0.01$; No symbol: not significant; Scale bar: 200 μm.

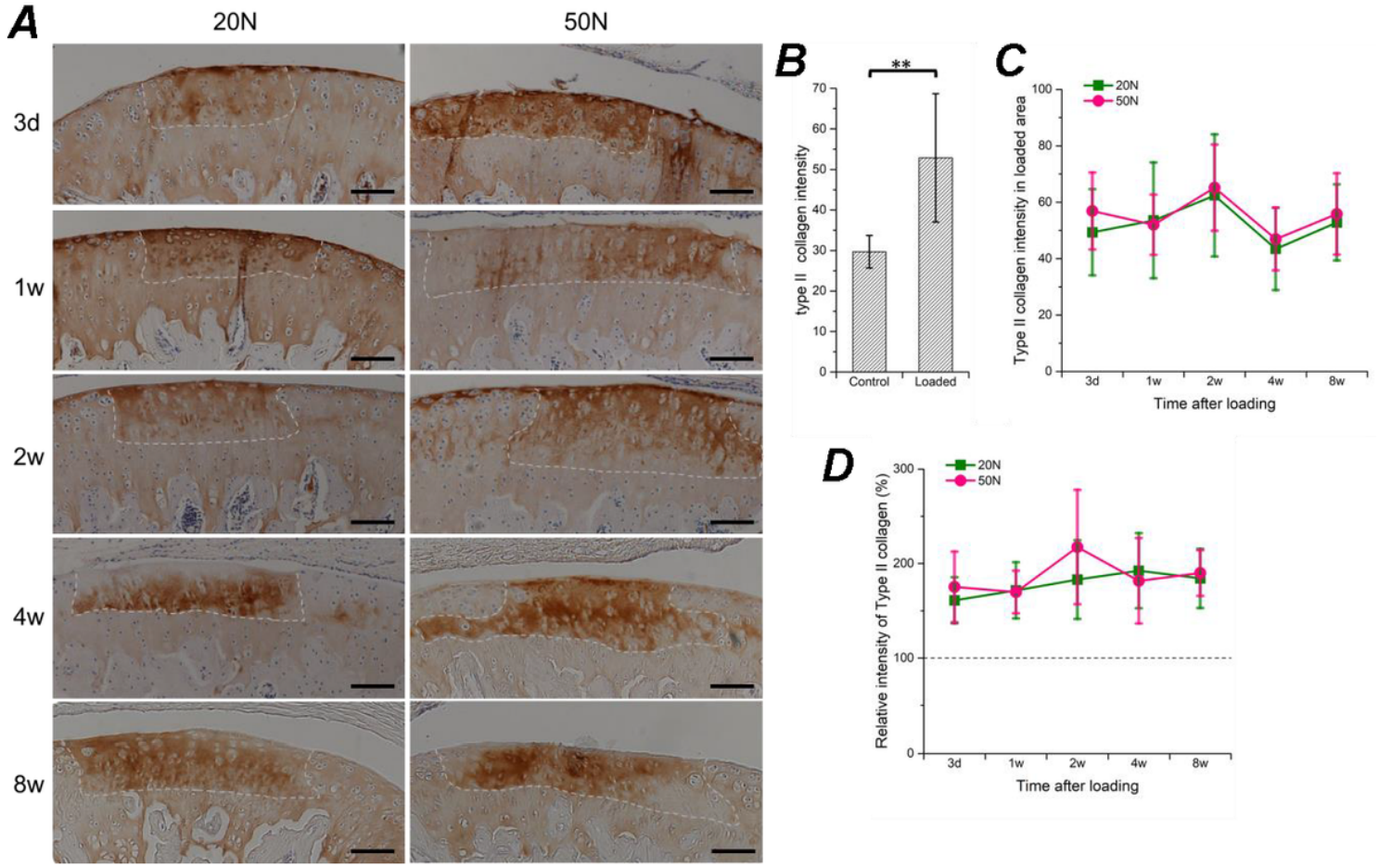

Figure 4

Changes in Type Ⅱ collagen expression in articular cartilage substrates after cyclic loading. Legends: A. Representative immunostained sections for type Ⅱ collagen in the lesion areas of lateral condyle cartilage. The border of normal and degenerative cartilage is represented by a dashed, light-grey line. B. Differences of Type Ⅱ collagen expression in Control and Loaded samples. C. Average intensity of staining on the degenerative cartilage matrix was calculated on 8-bit grey scale images using ImageJ software. D.

Percentage variation of intensity in the lesion area relative to the intact area on the same section. The relative intensity was calculated in an inverted 8-bit grey scale image by dividing the intensity in the intact area. Error bars represent standard deviation; No significant effect or interaction between time points or load levels; **p<0.01; No symbol: not significant; Scale bar: 100 μm.

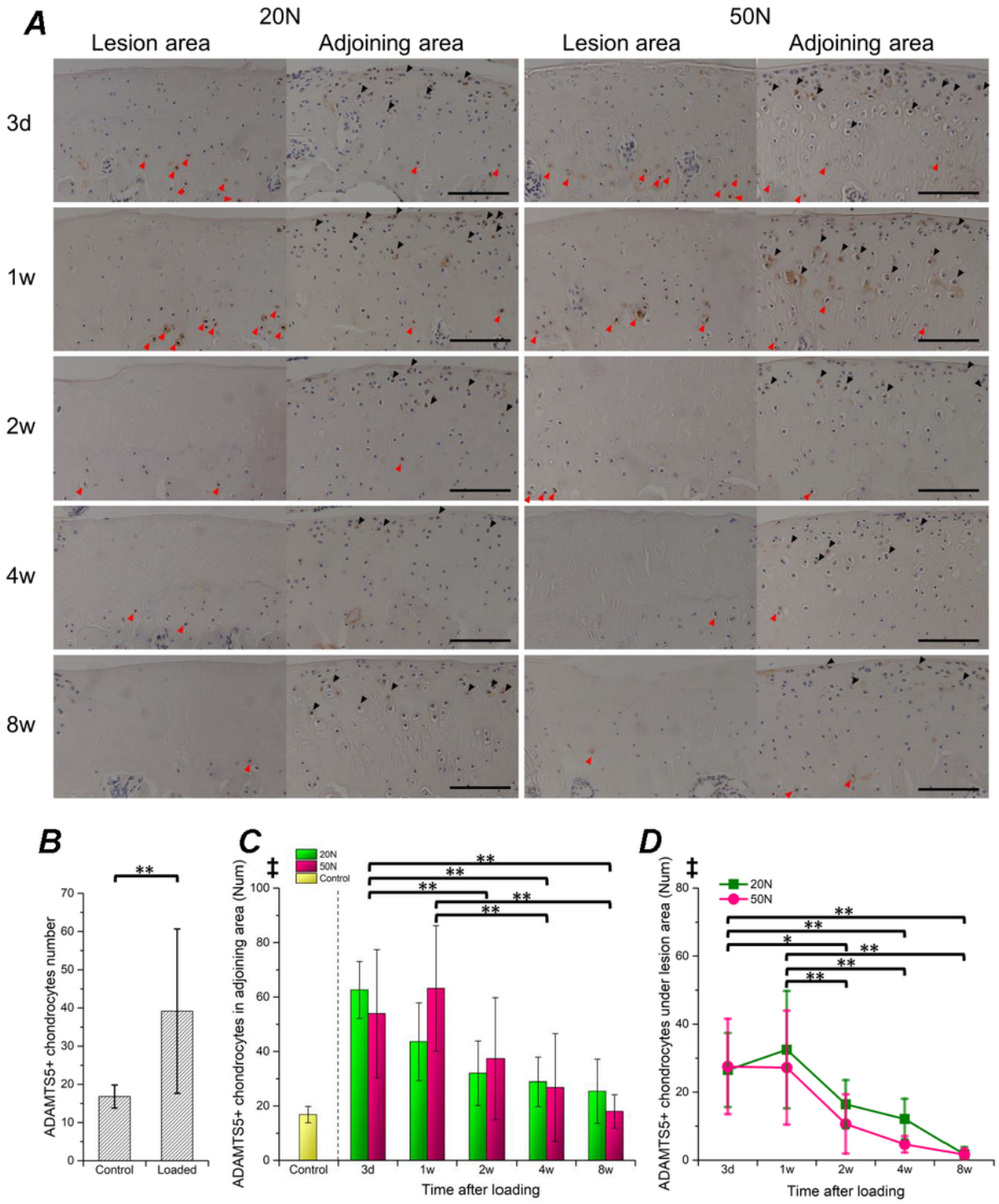

Figure 5

Distribution of ADAMTS-5+ chondrocytes in articular cartilage. Legends: A. Representative histological sections immunostained for ADAMTS-5+ in the lesion area and the adjoining zone. Black arrow heads indicate positive cells in the superficial and intermediate zone of cartilage, red arrow heads indicate positive cells under the tidemark. B. Comparison of positive cells number in intact cartilage with loaded cartilage (adjoining area). C, D. Results of semi-quantitative analysis of positive cells within the adjoining (C) and under the lesion area (D). Results were normalized by dividing by the cartilage surface length (mm). Error bars represent standard deviation; Significant results ($p<0.05$) of two-way ANOVA analysis are presented on the top of each chart; ‡: main effect of duration; Marginal means of each observational point was compared when ‡ was found.*$p<0.05$, **$p<0.01$; Scale bar: 100 μm.

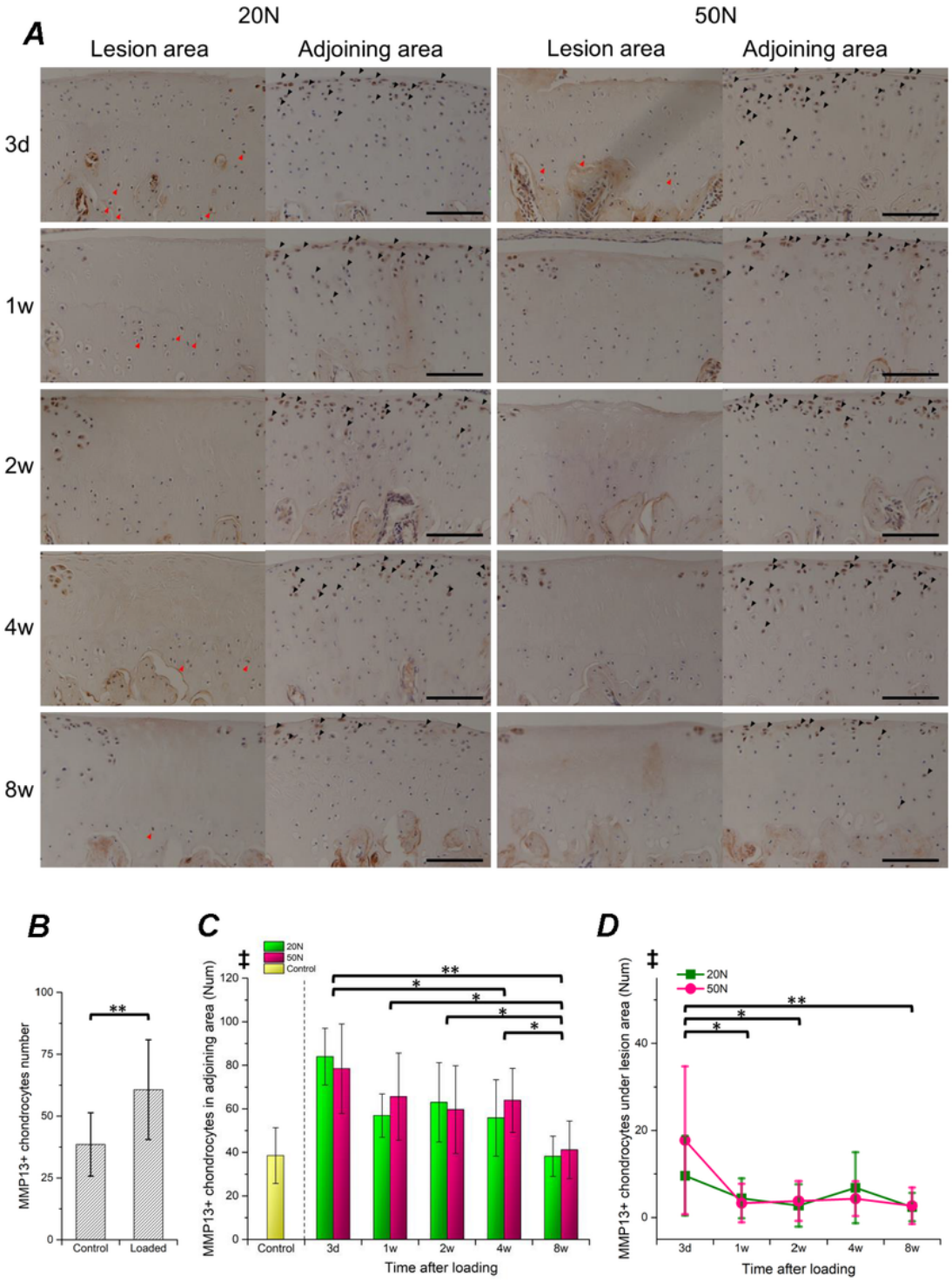

Figure 6

The distribution of MMP-13+ chondrocytes in articular cartilage. Legends: A. Representative histological sections immunostained for MMP-13+ in the lesion area and the adjoining zone. Black arrow heads indicate positive cells in the superficial and intermediate zone of cartilage, red arrow heads indicate positive cells under the tidemark. B. Comparison of positive cell number in intact cartilage with all loaded samples' adjoining area. C, D. Results of semi-quantitative analyses of positive cells within the adjoining

(C) and under the lesion area (D). Results were normalized by dividing by the cartilage surface length (mm). Error bars represent standard deviation; The significant results ($p<0.05$) of ANOVA analysis ‡: main effect of duration was presented on the top of each chart. Marginal means of each observational point was compared when ‡ was found.*$p<0.05$, **$p<0.01$; Scale bar: 100 μm.

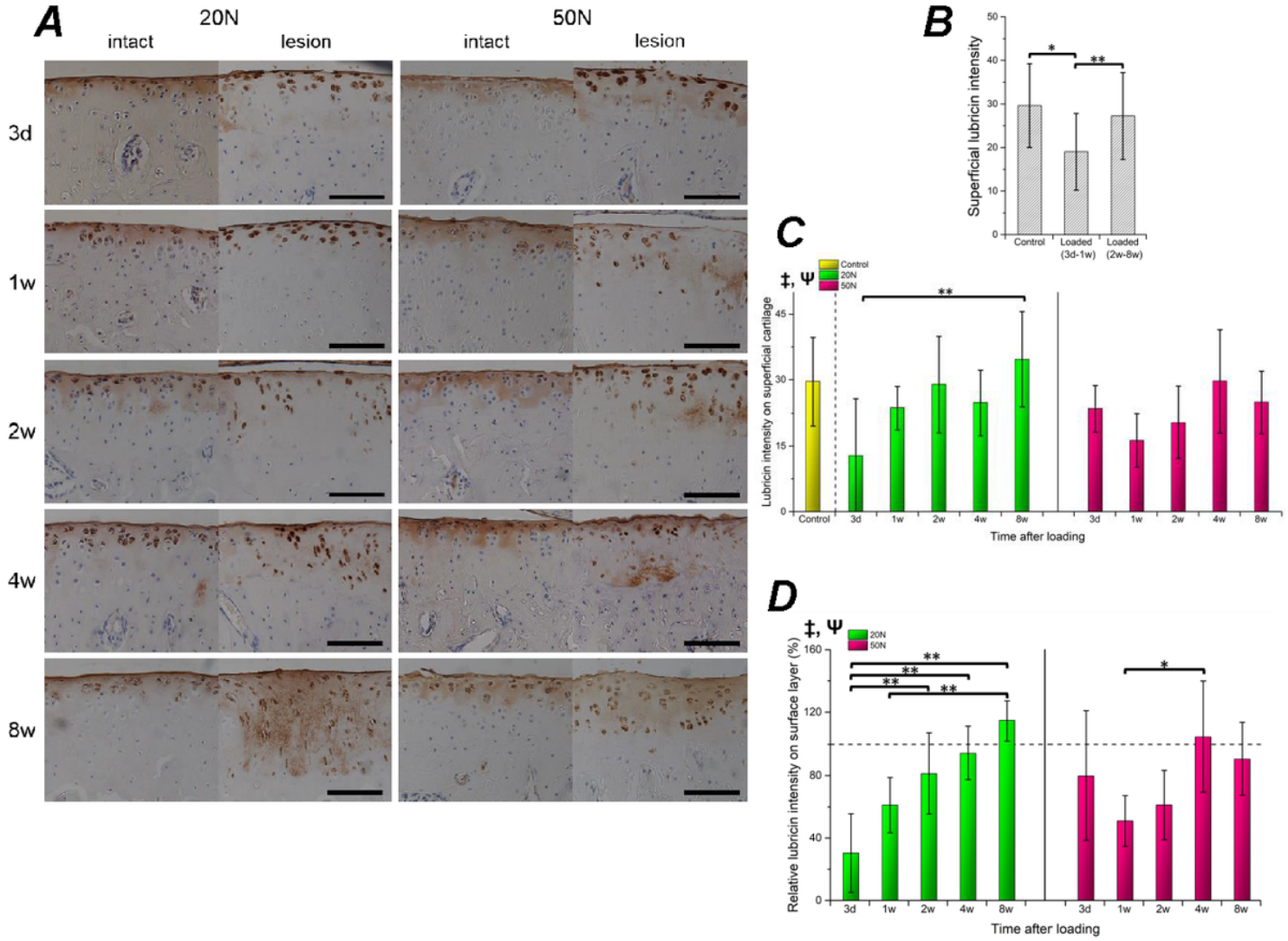

Figure 7

The localization of lubricin in articular cartilage subjected to dynamic loading. Legends: A. Representative Lubricin/Proteoglycan4 immunostained image in the lesion area of lateral condyle and intact area under the lateral meniscus. The staining weakened in the superficial substrates, whereas, it was enhanced in the cartilage lacunae. B. Differences of Control (n=6), early observation (3 days & 1 week; n=24) and later observation (2, 4, and 8 weeks; n=36) of loaded samples were compared using Kruskal-Wallis H tests. C. The staining intensity in the superficial layer of cartilage substrates. The ROI of superficial cartilage were depicted using ImageJ software using brush selection tool of 50 μm width (Supplementary figure 4). D. The relative intensity normalized with intact region staining in percentage. Significant results ($p<0.05$) of a two-way ANOVA analysis are presented on the top of each chart; ‡: main effect of duration, Ψ:

interaction effects; Stratified one-way ANOVA on each load level with multiple comparison were applied whenever Ψ was found. *p<0.05, **p<0.01; No symbol: not significant; Scale bar: 100 μm.

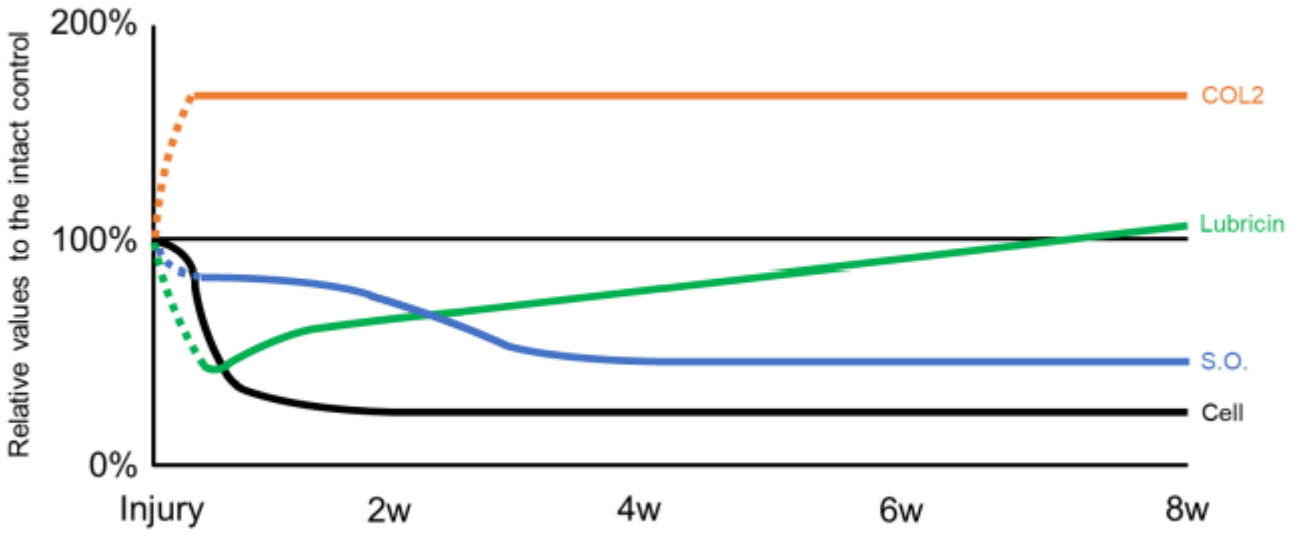

Figure 8

The illustration summarizes the findings of the current study. Localized Col2 upregulated within 3 days after loading and stable during observation. Superficial lubricin decreased immediately after damage yet recovered gradually to the normal level. The Safranin O staining in lesion cartilage weakened continuously after injury until the 4th week. Hematoxylin stained nuclei in the damaged area dissolved completely 2 weeks after cyclic compression.

Supplementary Files

This is a list of supplementary files associated with this preprint. Click to download.

- Supplementaryfigure.2.docx
- Supplementaryfigure.1.docx
- Supplementaryfigure.4.docx
- Supplementaryfigure.3.docx